Momentum and Energy Transfer between Coupled Mass-Spring Chains

Henry Jacobs

June 3, 2009

1 Introduction

In this paper I hope to illustrate how variational integrators can be used in the study of momentum and energy transfer, perhaps as a means to understand friction and dissipation. We will first be looking at a system of two colliding mass-spring chains, denoted C_t for the top chain and C_b for the bottom chain. The particles between chains are coupled by a nonlinear potential V_2. This creates a repulsive force making the model reminiscent of elastic collisions. All the springs are linear with spring constant k, and all masses are equal with masses $m_t = m_b = 1$. In the final section will will switch the nonlinear coupling into an attractive force and study how C_t transmits the energy to C_b from a random perturbation of a stable equilibrium. This last idea is intended to model heat.

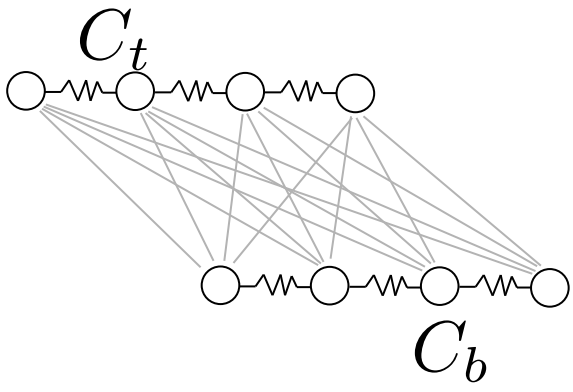

Figure 1: A schematic diagram of the model to be studied. The gray lines represent the nonlinear coupling between the chains.

Rather than showing videos, the information from a given trial can be easily shown in a 2d plot of time versus position. Figure 2 depicts the positions of the masses in a typical collision.

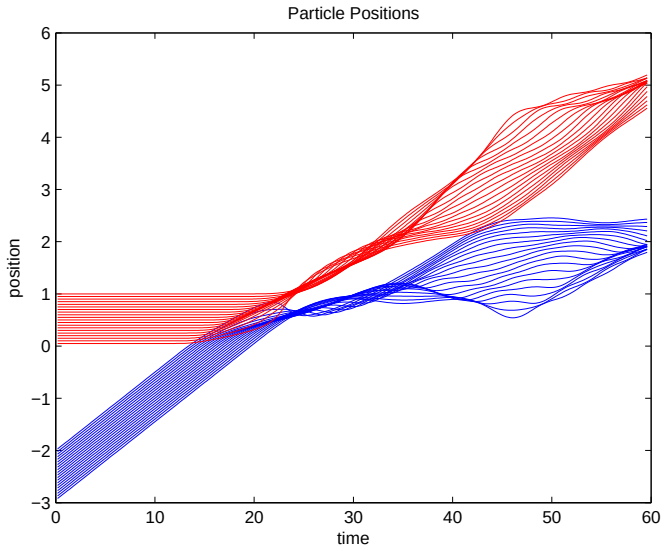

Figure 2: A typical collision of C_t and C_b. The red lines depict the position of the masses in C_b, while the blue lines depict the position of the masses in C_t. One can observe a mixture of standing and traveling waves which form after the collision.

Through numerical experiments and comparison with hard-ball systems we attempt to understand if and how this system can produce friction-like behavior.

2 The Model

As shown in the schematic diagram of figure 1 we have two mass-spring chains of n masses, C_t and C_b. We will ignore the possibility of hardball-collisions [1].

[1]Ignoring hardball collisions and using the potential V_2 given in our model is qualitatively similar to using a Morse potential and restricting the y-coordinate of C_t to be 1 and that of C_s to be 0. Such a restriction in a Morse potential would prevent particles from getting near the singularity at 0 and the experienced potential of one particle from the point of view of another will "look" like a smooth bulge with exponential radial decay.

2.1 Equations of Motions

Let $q_t, q_b \in \mathbb{R}^n$ store the positions of particles in C_t and C_b respectively. The potential energy from the linear springs is given by

$$V_1(q_t, q_b) = \frac{k_1}{2} \sum_{i=1}^{n-1} (q_t^{i+1} - q_t^i - l)^2 + (q_b^{i+1} - q_b^i - l)^2$$

Where l is the natural length of the spring, by default we set this to $\frac{1}{N}$. By default we set the spring constant $k_1 = 1.0$. The potential energy for the coupling between C_t and C_b will be

$$V_2(q_t, q_b) = k_2 \sum_{i,j=1}^{n} \exp\left(\frac{-(q_t^i - q_b^j)^2}{2\sigma^2}\right)$$

By defaults we set $k_2 = 0.001$. From observation a higher k prevents a lot of interesting interaction for initial velocites less than 1. Together, these potential functions give the total potential energy of $V = V_1 + V_2$. The mass of the each particle is simply $m = 1$ and so our kinetic energy can be written

$$K = \frac{m}{2}\|\dot{q}\|^2$$

We construct the Lagrangian

$$L(q, \dot{q}) = K(\dot{q}) - V(q)$$

The Euler-Lagrange equations are the familiar equations of motion for a particle in a potential,

$$m\ddot{q} + \nabla V(q) = 0$$

Explicity these are

$$m\ddot{q_t^l} + k_1(q_t^{l+1} - 2q_t^l + q_t^{l-1}) + k_2 \left(\sum_{j=1}^{n} \frac{1}{\sigma^2}(q_t^l - q_b^j) \exp\left(\frac{-(q_t^l - q_b^j)^2}{2\sigma^2}\right)\right) = 0$$

and similarly for q_b^l

$$m\ddot{q_b^l} + k_1(q_b^{l+1} - 2q_b^l + q_b^{l-1}) - k_2 \left(\sum_{i=1}^{n} \frac{1}{\sigma^2}(q_t^i - q_b^l) \exp\left(\frac{-(q_t^i - q_b^l)^2}{2\sigma^2}\right)\right) = 0$$

2.2 Conservations of Momentum

As an exercise we show explicitly how to show conservation of linear momentum. It's easy to see that the continuous system is invariant under the action of the group $G = \mathbb{R}$ of uniform translations in position, simply substitute $\phi_r(q^l) = q^l(t) + r$ into the Lagrangian (allowing for the abuse of notation that $q + r$ is the vector $q^i_{t,b} + r$).

$$L(q + r, \dot{q}) = \frac{m}{2}\|\dot{q}\|^2 - V(q + r)$$

and use that

$$\begin{aligned} V_1(q + r) &= \frac{k_1}{2}\sum_{i=1}^{n-1}((q_t^{i+1} + r) - (q_t^i + r) - l)^2 + ((q_b^{i+1} + r) - (q_b^i + r) - l)^2 \\ &= \frac{k_1}{2}\sum_{i=1}^{n-1}(q_t^{i+1} - q_t^i - l)^2 + (q_b^{i+1} - q_b^i - l)^2 \\ &= V_1(q) \end{aligned}$$

and that

$$\begin{aligned} V_2(q + r) &= k_2\sum_{i,j=1}^{n}\exp\left(\frac{-((q_t^i + r) - (q_b^j + r))^2}{2\sigma^2}\right) \\ &= k_2\sum_{i,j=1}^{n}\exp\left(\frac{-((q_t^i + r) - (q_b^j + r))^2}{2\sigma^2}\right) \\ &= V_2(q) \end{aligned}$$

We see that the exponential map from the lie-algebra $\mathfrak{g} = \mathbb{R}$ is $\exp(\xi) = \xi$, thus infinitesimal generator for $\xi \in \mathfrak{g}$ is

$$\xi_Q = \begin{pmatrix} \xi \\ \vdots \\ \xi \end{pmatrix}$$

The corresponding momentum map $J : TQ \to \mathfrak{g}^*$ satisfies

$$\langle J(q, \dot{q}), \xi\rangle = \langle \mathbb{F}L(q, \dot{q}), \xi_Q\rangle$$

Where the fiber derivative $\mathbb{F}L = \frac{\partial L}{\partial \dot{q}}$ in this case. Putting together the pieces we find

$$J(q, \dot{q}) = \dot{q}^T M \cdot \begin{pmatrix} 1 \\ \vdots \\ 1 \end{pmatrix} = \sum_i m\dot{q}^i$$

We will see later that the analogous arguments for discrete mechanics produce a slightly different discrete momentum.

3 Variational Integrators

A variational integrator is formed by maximizing an approximation of the action integral, rather than working with the Euler-Lagrange equations directly. Assuming the configuration manifold is a vector space, we can approximate the Lagrangian $L : TQ \to \mathbb{R}$ with $L_d : Q \times Q \to \mathbb{R}$ defined by

$$L_d(q_1, q_2) = L(\frac{q_1 + q_2}{2}, \frac{q_2 - q_1}{\Delta t})$$

Where Δt is some sufficiently small interval of time. We then define the discrete action integral

$$S_d[q] = \sum_{k=1}^{N-1} L_d(q_k, q_{k+1})$$

Which upon setting $\frac{\partial S_d}{\partial q_k} = 0$ we find

$$D_1 \cdot L_d(q_k, q_{k+1}) + D_2 \cdot L_d(q_k, q_{k+1}) = 0$$

A trajectory $[q] = \{q_k\}_{k=1}^{N}$ that satisfies the above equation will maximize $S_d[q]$, and hence approximately maximize the action integral of the continuous system over short periods of time (a concern of backward error analysis).

In the case of the typical $L = K - V$ type of Lagrangian the discrete Euler-Lagrange equations are

$$M\left(\frac{q_{k+1} - 2q_k + q_{k-1}}{h^2}\right) + \frac{1}{2}\left(\nabla V(\frac{q_{k+1} + q_k}{2}) + \nabla V(\frac{q_k + q_{k-1}}{2})\right) = 0$$

This is the method we implement on the Lagrangian explained in section 2 (See the Appendix for code).

3.1 Conservation of Discrete Momentum

As an exercise I'll explicitly show the symmetry that will give conservation of linear momentum for the system. Let our group be $G = \mathbb{R}$. We define the action on Q to be

$$\Phi_g(q) = q^i + g$$

That is, we just add g to each coordinate. The action on $Q \times Q$ is simply $\Phi(q_0, q_1) = (\Phi(q_0), \Phi(q_1))$. It's easy to see that this action leaves L_d invariant.

$$\begin{aligned} L_d(q_1 + r, q_2 + r) &= L(\frac{(q_1 + r) + (q_2 + r)}{2}, \frac{(q_2 + r) - (q_1 + r)}{\Delta t}) \\ &= L(\frac{q_1 + q_2}{2} + r, \frac{q_2 - q_1}{\Delta t}) \end{aligned}$$

because Φ leave L invariant

$$\begin{aligned} &= L(\frac{q_1+q_2}{2}, \frac{q_2-q_1}{\Delta t}) \\ &= L_d(q_1, q_2) \end{aligned}$$

The lie algebra is again $\mathfrak{g} = \mathbb{R}$, and the exponential map is $\exp(\xi) = \xi \in G$. The infinitesimal generator from Φ is

$$\xi_{Q\times Q} = \begin{pmatrix} \xi \\ \vdots \\ \xi \end{pmatrix}$$

, In the arena of discrete mechanics this symmetry implies a discrete momentum map satisfying

$$J^-_{L_d}(q_0, q_1) \cdot \xi = \langle \Theta^-_{L_d} L_d, \xi_{Q\times Q} \rangle (q_0, q_1)$$

Where $\Theta^-_{L_d}$ is the minus discrete Lagrangian one form [1]. In this case

$$\Theta^-_{L_d} L_d = \frac{-1}{\Delta t^2}(q_1 - q_0)^T M - \frac{1}{2} dV\left(\frac{q_1+q_0}{2}\right)$$

So that $J^-_{L_d}$ is

$$J^-_{L_d}(q_0, q_1) = \sum_i \frac{1}{h^2} m(q_1^i - q_0^i) + \frac{1}{2} dV^i\left(\frac{q_1+q_0}{2}\right)$$

Not quite what I'd expect. If you caught me off-guard I'd expect the momentum to be $J_{guess} = \frac{m}{h}\sum_i (q_1^i - q_0^i)$, but this is not quite conserved by the algorithm. Although J_{guess} does seem to oscillate quite rapidly with low amplitude (like 10^{-14}) about a constant value, and doesn't bias towards any one direction. This is likely related to what occures when we take the continuum limit of the discrete momentum times the time-step h. If $q_1 = q(h+t)$ and $q_0 = q(t)$ we see

$$\lim_{h\to 0}(h \times J_d(q(t+h), q(t)) = \sum_i m\dot{q}^i + 0 = J(q, \dot{q})$$

4 Numerical Performance

We start in an arrangement where all the particles within each chain are spaced l apart (This is the equilibrium arrangement when V_2 is absent). We make a series

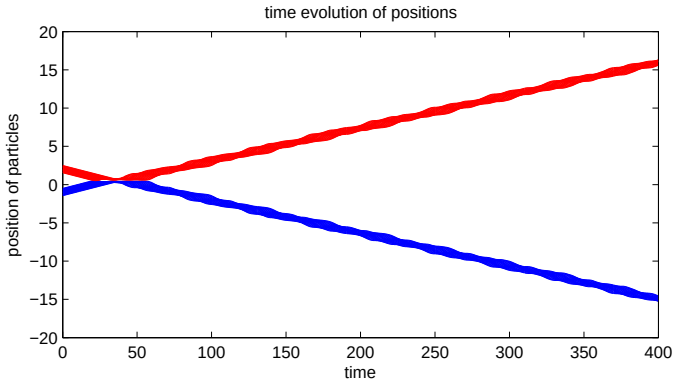

Figure 3: Depicts the position of the particles. Red is for C_b and blue is for C_t, it appears I mismatched my label so that C_t is below C_b.

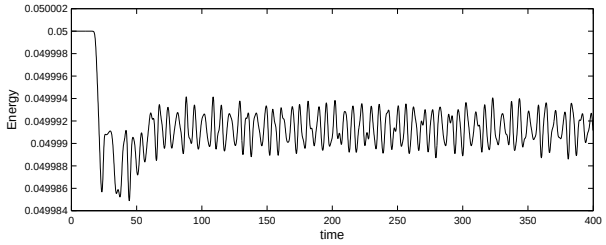

Figure 4: Energy Preservation properties, Note the scale on the y-axis. The largest change in total energy is 3.3944×10^{-04} of the largest change in potential energy.

of observations on the quality of the integrator for C_t and C_b initially separated by a distance of 3, heading towards each other with an initial velocity $v_0 = 0.1$ and. The evolution of the particles is depicted in figure 3

We observe that the algorithm does a very good job of preserving energy and symmetries. Figure 4 depicts how energy evolves in time.

to find $\phi^* L = L$. This gives us conservation of linear momentum via Noether's theorem. This is shown to hold for a general system of N particles on the configuration manifold $Q = \mathbb{R}^{3N}$ in [1], section 11.4. The momentum map is found to be $J(\xi_r)(q,p) = \sum p$. In the discrete case we notice that L_d is invariant under the same symmetry since Thus L_d is invariant as well and we can apply the discrete Noether's theorem as described in [2]. We get a discrete momentum map

$$\sum_i \frac{1}{h^2} m(q_1^i - q_0^i) + \frac{1}{2} dV^i \left(\frac{q_1 + q_0}{2} \right)$$

We observe the conservation of this momentum in figure 5. The approximation of J_{guess} mentioned early was found to oscillate about a constant value with make deviation on the order of 10^{-14}.

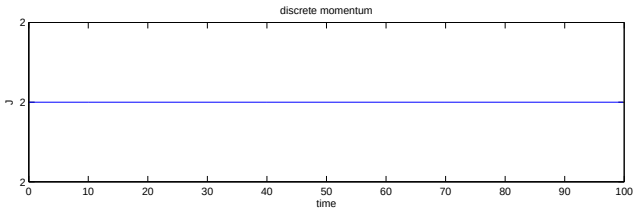

Figure 5: Illustration of Momentum Preservation, it appears it's of machine precision from the looks of the scale on the y-axis

Additionally since we've set the initial conditions equal modulo space translation, this system should exhibit a symmetry when moving in a frame with the center of mass with each spring chain separately as a result of conserving linear momentum. For fun's sake we can literally observe symmetry in figure 6 noting how both wobble equal and opposite to each other, even after very long times.

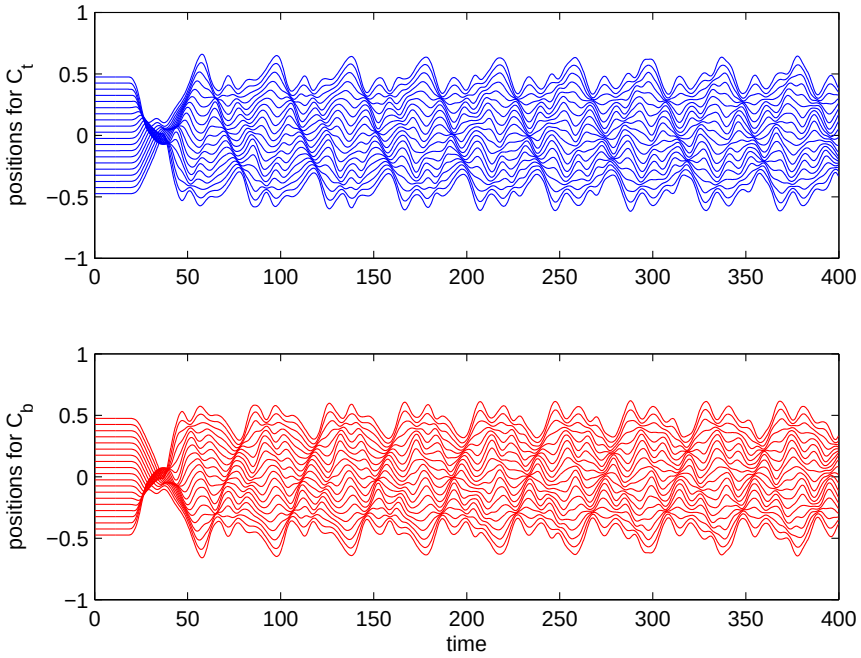

Figure 6: The top plot depicts positions of particles of C_t in a frame that moves with its center of mass. The lower plot does this for C_b.

5 A Hypothesis on Friction and Kinetic Theory

In this section I'm going to take a stab at explaining of Rayleigh friction in a hard-ball system using conservation of energy and momentum, I don't have any references for this, and would invite input here. Nonetheless some of the thinking used here leaks into the next section so I chose to include it for the sake of understanding motivations later.

In a perfectly elastic collision between billiard balls momentum $p = m_1 v_1 + m_2 v_2$ and energy $E = \frac{m_1}{2} v_1^2 + \frac{m_2}{2} v_2^2$ are both conserved. This is enough info to solve for the velocities after the collision. For simplicity assume v_2 is normally distributed with mean 0. Let the velocity of ball 1 after collision be v_1^f. The expected value of v_1^f is

$$\langle v_1^f \rangle = \langle \frac{v_1(m_1 - m_2) + 2m_2 v_2}{m_1 + m_2} \rangle = v_1 \frac{m_1 - m_2}{m_1 + m_2}$$

This tells us how a collision will change velocity. After 500 collision we should expect a velocity of

$$\langle v_1^{(f,500)} \rangle = v_1 \left(\frac{m_1 - m_2}{m_1 + m_2} \right)^{500}$$

The definition of temperature used in kinetic theory is proportional to the collision rate of the molecules. Let $C = \alpha T$ be the collision rate. Thus we expect $C\Delta t$ collisions in a time Δt. If $\langle v(t) \rangle$ is the expected velocity of ball 1 at time t we expect the velocity at time $t + \Delta t$ to be

$$\langle v(t + \Delta t) \rangle = \left(\frac{m_1 - m_2}{m_1 + m_2} \right)^{\alpha T \Delta t} \langle v(t) \rangle$$

Taking the logarithm on both sides and rearranging we get

$$\frac{1}{\Delta t} (\log \langle v(t + \Delta t) \rangle - \log \langle v(t) \rangle) = \alpha T \log \left(\frac{m_1 - m_2}{m_1 + m_2} \right)$$

Taking the limit as $\Delta t \to 0$ we get

$$\frac{d}{dt} \langle v(t) \rangle = \alpha T \log \left(\frac{m_1 - m_2}{m_1 + m_2} \right) \langle v(t) \rangle$$

Assuming $m_1 > m_2$ then

$$\alpha T \log \left(\frac{m_1 - m_2}{m_1 + m_2} \right) < 0$$

and the dynamics of $\langle v \rangle$ are the same as $\ddot{q} = -\gamma \dot{q}$, the standard friction law.

6 Momentum Transfer

Just as in the hard ball system we observe transfers of momentum in our system. The average momentum of each chain after each collision is a little less than it was before perhaps due to internal motion of each of the chains. See figure 7

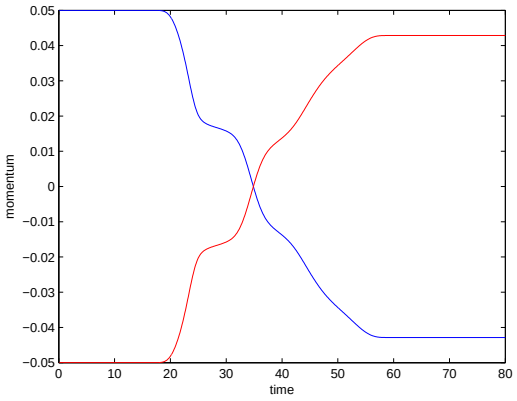

Figure 7: An example of transfer of linear moment from C_t to C_b, observe that both emerge with angular momentum closer to the average after the collision. In this case the average is 0.

We now show results of some numerical experiments and attempt to connect them to the analysis done in the section on kinetic theory. One of the requirements to mimic the momentum transfer mechanism of the previous section is that the percent change in speed resulting from a collision be independent of the pre-collision velocity. In the last section that percentage was always $\frac{m_1-m_2}{m_1+m_2}$ regardless of velocity. I ran the model at various pre-collision velocities to see if this is the case. It appears not, see figure 8

If collisions could in some way be interpreted as producing Rayleigh friction (upon taking a continuum limit), it would need to be in a way fundamentally different from the hard-ball system, since the momentum change appears to be velocity dependent here. We can start by first considering two fundamental differences between collisions of C_t and C_b vs collision of billiard balls. The first is that the momentum transfer for billiard balls depends solely on shape, energy, and momentum, and the solution becomes ill-conditioned as curvature increases. In contrast our system uses a smooth potential to do the momentum transfer and the particles have no shape at all, they are points (infinite curvature, if that's meaningful). In fact our particles can pass through each other. If one passes through

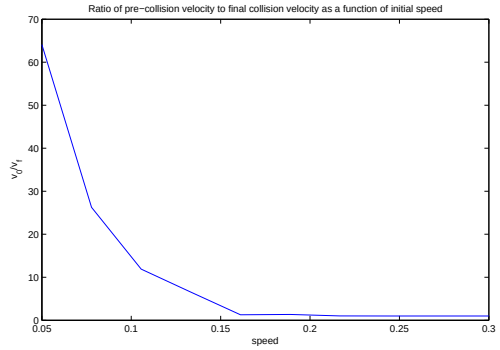

Figure 8: Ratio of initial to final velocity for various velocities.

another at a speed v both will experience an impulse from V_2 proportional to the time spent close to one another. This time spent is inversely proportional to v, and provides one hypothesis as to why figure 8 looks a bit like $\frac{1}{v}$. This also suggests that in order for a potential to mimic the "friction" I interpreted from the hard-ball system requires a singularity somewhere. A potential with a singularity may have the property that moving at higher speeds is countered by a steepening potential and can produce a change in momentum that doesn't decrease with increased speeds. Additionally, such a singularity would make it impossible for particles to pass through each other. The second difference is that the billiard balls practice elastic collisions, while C_t and C_b have internal degrees of freedom, and if you close your eyes to those degrees of freedom the collisions will appear inelastic. This difference is a bit less dramatic, but should result in a superficially faster than expected loss of average momentum and energy of C_t and C_b (again, with eyes closed to there internal dynamics, the full system is still conservative and momentum preserving).

7 Modeling Heat

One idea worth investigating further is how to use mass-spring chains to model heat. A popular model from solid state physics is known as the Frenkel-Kontorova Model (FKM) where a chain of masses is dragged over a substrate with sinusoidal potential. The model exhibits lots of interesting behavior. It serves as a means of modeling material impurities and kinks in crystal lattices among about a thousand other things. In the continuum limit the FKM becomes the Sine-Gordon equation (SGE) which we know to be a Hamiltonian system with soliton solutions, which exist in the analogous form in the FKM. Despite the complete integrability of the SGE, such tidiness does not flow down to the FKM, as the discrete complexities

become possible. It is known that the FKM is capable of producing Rayleigh friction if one tries to include the unknown internal dynamics of the substrate through a stochastic transition operator (see [3], chapter 7). A diagram of the original FKM is shown in figure 9.

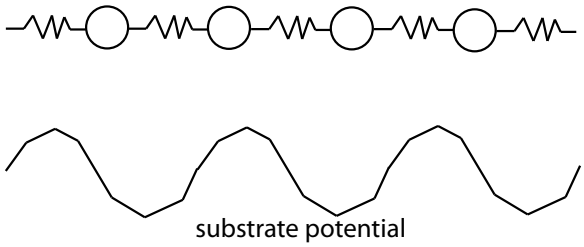

Figure 9: A diagram of the Frenkel Kontorova model. In the original model the substrate potential is independent of the motions of the masses.

Here we consider C_b our substrate, bearing the flavor the FKM model. We place C_t above C_b in a stable equilibrium so that total energy is zero and the masses are in a potential well. We then then add a random perturbation to the particles of C_t so that the energy of the system can be completely attributed to this random perturbation. Upon running the integrator we can view if and how this energy is exchanged to C_b in a deterministic way (the only thing random is the initial condition). First we must find a stable equilibria to perturb.

7.1 Finding Stable Initial Conditions

Finding a stable initial condition amounts to finding where $\nabla V = 0$. This problem is probably not analytically solvable, and fails to converge under Newton-Raphson from singular derivatives. In order to find an equilibria I added a weak friction force by apending the term $\frac{1}{\Delta t}(q_2 - q_1)$ to the Discrete-Euler Lagrange equations. This dissipative system will guide trajectories towards an equilibrium of the system. Upon re-substituting this computed equilibrium into the original conservative system I observed it to be stable.

7.2 Numerical Results of the Heat Model

Given the stable initial condition q_0 we add a normally distributed vector with the average adjusted to 0 to the C_t part of q_0 to get q_1 in an attempt to model thermal noise. The idea is that C_t will be "hot", and C_b will be "cold". The particles trajectories of C_t should look very disordered to the naked eye. We then run the

simulation and observe if and how energy is transferred from C_t to C_b through the non-linear coupling. The positions of the masses is shown in figure 10

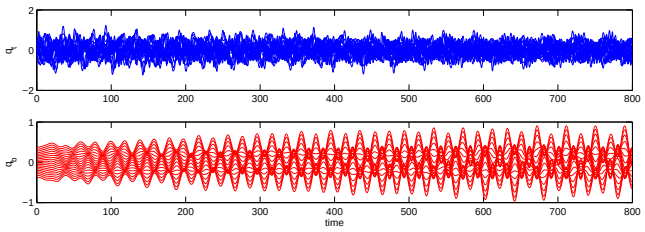

Figure 10: Time Evolution of mass positions. C_t is blue, intended to be the "hot" substrate, while C_b in red is intended to be the cold substrate. We observe a slow transfer of kinetic energy to C_b, it appears to only be absorbing certain resonant frequencies.

I do not observe a "heat-like" energy transfer. The energy dynamics are depicted in figure 11. The energy settles but doesn't equilibrate. The oscillations in C_t are pretty wild. The power spectrum of the signals $q_t(t)$ and $q_b(t)$,the positions in the top and bottom chains respectively, can shed some light. We show the power spectrum in figure 12

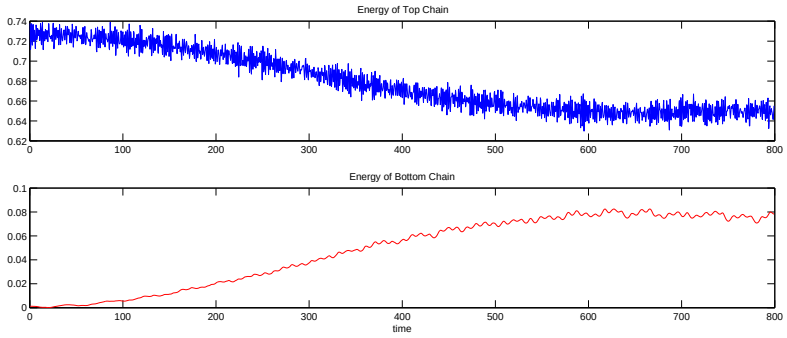

Figure 11: Energy transfer from C_t to C_b is slow, and does not seem to settle to an even distribution between C_t and C_b. For reassurance, my time step is about one tenth the natural frequency

It seems energy is trapped in high-frequency modes. Roughly speaking, as a mass q_t of C_t wobbles by a mass q_b of C_b, the potential V_2 only "turns on" in a region of size σ. Similar to the argument made in section 6, explaining why the change

in velocity after a collision appeared $\sim v^{-1}$. If q_t is in this region for a time-span t then by equating impulse with change in momentum, it can alter the momentum of q_b by an amount $\sim t$. If q_t is dominated by high frequency signals, then $t \sim f^{-1}$ is bound to be really small, and change in momentum follows $\Delta p \sim f^{-1}$ is small as well.

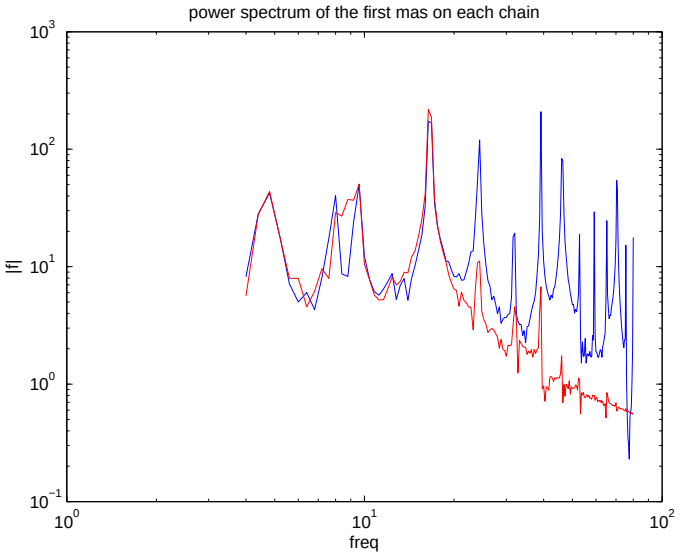

Figure 12: We observe that for the most part, $\|\hat{q}_t^1\|$ and $\|\hat{q}_b^1\|$ are relatively close at low frequencies, and the resonant modes nearly match. At the higher frequencies the energy seems stuck in C_t.

8 Future Work

We have seen that variational integrators serve as a great tool for analyzing the intricacies of momentum and energy transfer between coupled systems. Possible future directions for this project would be to get a better grasp on the analytical side of inelastic collisions and the friction like properties of the FKM and the ramifications of random initial conditions. Unfortunately I learned too recently how to begin to deal with this. We begin with a density $\rho(q_t, q_b, \dot{q}_t, \dot{q}_b)$, the one we've chosen in the section on heat would be a product of normal distribution for the C_t part and impulse functions for the C_b part. Then we note that the

distribution evolves according to

$$\frac{\partial \rho}{\partial t} = -\{\rho, H\}$$

Where we've converted to the poisson bracket form of the system [4], which we could just as easily pullback to the Langrangian side. Then the expected value for the energy of C_b would be

$$\langle E_b \rangle = \int_Q \left(\frac{m}{2} \|\dot{q}_b\|^2 + V_{b,springs}(q_b) \right) \rho(q) dQ$$

and it would evolve in time according to

$$\frac{d}{dt}\langle E_b \rangle = \langle \frac{\partial V}{\partial q_b} + dV_{b,springs} \rangle + \int_Q (\frac{m}{2} \dot{q_b}^2 + V_{b,springs}(q_b)) \frac{\partial \rho}{\partial t} dQ$$

The details for the distribution i've chosen seem to propagate complexity, and I'm not done working through it yet. Additionally I have some concerns with the non-homogenous nature of finite mass spring chains. A way to amend this is to use rings instead, i.e. a model of two rings of mass springs constrained to a distance of 1 from each other but free to rotate, this could be easily modified to mimic the FKM with periodic boundary conditions. I initially wanted to do something like this. I got bogged down in debugging, and an overly complex choice of integrator. So for now I chose to compromise in the interest of time. I suspect I'm close to getting the two ring model off the ground soon though. For comparison with hard ball systems, using different potentials (ones with a singularity at the origin) should produce different results, and the dependence on the shape of the potential in general seems like a fun problem. A simultaneous though less urgent pursuit would be trying to understand the connection between friction and randomness, which at the moment is just a notion for me.

9 Appendix: Matlab Code

Here's the program I used to implement the scheme outlined in section 2.

```
function [q,t,K,K_b,K_t,V,V_b,V_t,p_b,p_t] = model11(v0)
% Simulates two Hookean mass spring chains with
% a nonlinear coupling between each other.  The
% positions of the masses are stored in the vector q.

global N l k k_a sigma
N = 20;
l = 1./N;
k = 1.0;  % spring constant
k_a = 0.001; % coupling (+ for repulsion)
sigma = 0.1;
mt = 1.0;  % mass of springs on top
mb = 1.0;  % mass of springs below

M = [mt*eye(N) zeros(N);zeros(N) mb*eye(N)]; %mass matrix
h = min(2*pi./(10*sqrt(k)),0.1);    % time-step size
step_max = 1000;  %number of time steps to implement

% initial conditions
qt0 = (l.*(1:N)')-3;
qt1 = qt0 + h.*v0;
qb0 = l.*(1:N)';
qb1 = qb0;% - h.*v0./2;

% initialize q
q = zeros(2*N,step_max);
q(:,1) = [qt0;qb0];
q(:,2) = [qt1;qb1];

% run integrator
display('running integrator')
V = zeros(1,step_max-2);
V_t = zeros(1,step_max-2);
V_b = zeros(1,step_max-2);

K = zeros(1,step_max-2);
K_t = K;
K_b = K;
p_t = K;
p_b = K;
for ind = 3:step_max
    q1 = q(:,ind-1);
    q0 = q(:,ind-2);
    q2 = 2*q1-q0;
    error = 1;
```

```
    while error > 10^(-8)
        [V1,dV1,d2V1, Vt_1, Vb_1] = potential(0.5.*(q0+q1));
        [V2,dV2,d2V2, Vt_2, Vb_2] = potential(0.5.*(q2+q1));
        F = (1./(h^2)).*M*(q2-2.*q1+q0)+0.5.*(dV1+dV2);
        error = max(abs(F));
        q2 = q2 - ((1/h^2).*M+0.25*d2V2)\F;
    end
    q(:,ind) = q2;
    V(ind-2) = 0.5*(V1+V2);
    V_t(ind-2) = 0.5*(Vt_1+Vt_2);
    V_b(ind-2) = 0.5*(Vb_1+Vb_2);
    vel = (q2-q0)./(2*h);
    K(ind-2) = 0.5.*(vel'*M*vel);
    vel_t = vel(1:N);
    p_t(ind-2) = mean(mt*vel_t);
    K_t(ind-2) = 0.5*mt*(vel_t'*vel_t);
    vel_b = vel((N+1):(2*N));
    p_b(ind-2) = mean(mb*vel_b);
    K_b(ind-2) = 0.5*mb*(vel_b'*vel_b);
end
t = h.*(1:(step_max-2))';
store = q;
q = store(:,2:(end-1));

display('done integrating')
beep
end

function [V, dV, d2V, Vt, Vb] = potential(q )
%  [V, dV, d2V, Vt, Vb] = potential(q )
%  Gives the potential and fist and 2nd derivatives
%  of the potential function V = V_1 + V_2

global N k k_a l sigma

%-------------------------------------------
% HOOKEAN SPRINGS
% Here we construct V_1, dV_1, d2V_1
% The linear spring potential
%-------------------------------------------
TOEPb = spalloc(N,N,3*N);
TOEPb = spdiags(ones(N,1),0,TOEPb);
TOEPb = spdiags(-ones(N-1,1),-1,TOEPb);
TOEPb = TOEPb+TOEPb';    % Toeplitz Matrix
TOEPb(1,1) = 1;
TOEPb(N,N) = 1;
TOEPt = TOEPb;

qt = q(1:N); % top row
```

```
qb = q((N+1):2*N); % bottom row

dVb = k.*TOEPb*qb + [k*l; zeros(N-2,1);-k*l]; % bottom row springs
dVt = k*TOEPt*qt + [k*l;zeros(N-2,1);-k*l]; %top row springs

DIFF = speye(N);
DIFF = spdiags(-ones(N-1,1),-1,DIFF);
DIFF(1,1) = 0;

Vb = (k/2).*norm(DIFF*qb-l.*[0;ones(N-1,1)]).^2;
Vt = (k/2).*norm(DIFF*qt-l.*[0;ones(N-1,1)]).^2;

dV_1 = [dVt;dVb]; %diff pot from springs
V_1 = Vb + Vt; %potential from the springs
d2V_1 = [TOEPt zeros(N); zeros(N) TOEPb]; %2nd deriv pot

%-----------------------------------------
%  THE NONLINEAR COUPLING POTENTIAL
%  here we construct V_2, dV_2, D2V_2
%-----------------------------------------
Delta = repmat(qt,1,N)-repmat(qb',N,1);
V_mat = exp((-1/(2*sigma.^2)).*(Delta.^2));
V_2 = k_a.*sum(sum( V_mat )); %coupling potential

dV_2t = ((-k_a/(sigma^2)).*Delta.*V_mat)*ones(N,1);
dV_2b = ((k_a/(sigma^2)).*Delta.*V_mat)'*ones(N,1);
dV_2 = [dV_2t; dV_2b]; % diff coupling potential

d2V_2tt = diag( ((k_a.*( (-1/sigma^2))+(1./sigma^4).*Delta.^2 ).*V_mat)*ones(N,1) ) ;
d2V_2bb = diag( ((k_a.*( (-1/sigma^2))+(1./sigma^4).*Delta'.^2 ).*V_mat')*ones(N,1) ) ;
d2V_2tb = k_a.*V_mat.*((1/(sigma^2))-(1/sigma^4).*Delta.^2);

d2V_2 = [d2V_2tt d2V_2tb;d2V_2tb' d2V_2bb]; % 2nd deriv coupling pot.

%-----------------------------------------------------
%Here we sum things to get total potential and derivatives
%-----------------------------------------------------
V = V_1 + V_2;  %total pot
dV = dV_1+dV_2; %total diff pot
d2V = d2V_1 + d2V_2;    %2nd deriv pot
end
```

10 References

[1] J. E. Marsden & T. S. Ratiu, "Introduction to Mechanics and Symmetry: 2nd Edition", Springer, NY, 1999

[2] M. West, "Variational Integrators", Caltech, 2004

[3] O.M. Braun & Y.S. Kivshar, "The Frenkel-Kontorova Model", Springer, NY 2003

[4] R.C. Tolman, "The Principles of Statistical Mechanics", Dover, 1980